International Congress of Refrigeration
Sydney, Australia, September 19-24, 1999

FINNED -TUBE EVAPORATOR MODEL WITH A VISUAL INTERFACE

PIOTR A. DOMANSKI
National Institute of Standards and Technology
100 Bureau Dr., Stop 8631
Gaithersburg, MD 20899-8631, USA

ABSTRACT

This paper presents a finned-tube evaporator model and its utility when equipped with a window-based interface. The modeling scheme is "tube-by-tube" and allows for specification of complex refrigerant circuits, modeling refrigerant distribution between these circuits, and accounting for non-uniform air distribution. Evaporator capacity is obtained based on the simulated performance of each tube in the evaporator assembly using inlet parameters and mass flow rates of the refrigerant and air associated with a given tube. Simulation results also include local parameters for each tube such as inlet and outlet quality, temperature, enthalpy, entropy, pressure drop, mass flow rate for refrigerant and inlet and outlet temperature for air. The local data are displayed for each tube on a side view of the heat exchanger identifying tube connections, which facilitates a detailed understanding of the optimized evaporator's design.

1. INTRODUCTION

Finned-tube air-to-refrigerant heat exchangers are manufactured with a variety of refrigerant circuitry designs. Simulation models that account for refrigerant circuit architecture are better equipped for accurately predicting the heat exchanger performance. This is because the refrigerant path through the heat exchanger can have a significant effect on heat exchanger performance. The model presented here, EVAP5, originated in the tube-by-tube simulation model formulated by Chi (1979). Modifications and upgrades by Domanski and Didion (1983), Domanski (1991), and Lee and Domanski (1997) brought the model to its current capabilities. Current features of the model include the capability to simulate refrigerant distribution in the refrigerant circuit and to account for a one-dimensional maldistribution of air. EVAP5 employs REFPROP refrigerant thermophysical property routines and can be used with any refrigerant or refrigerant mixture for which properties can be calculated using the REFPROP package (Gallagher *et al.*, 1996).

For the model, the refrigerant circuitry information is a sequence of numbers identifying a feeder tube for each tube in the evaporator assembly. Coding refrigerant circuitry has proven to be an error-prone process that can effectively discourage the use of the program. For this reason, an interface was developed to facilitate the input and visual verification of the specified circuitry in a "windows" type of environment. This interface also proved to be very useful as a post processor of the simulation results by displaying local thermodynamic parameters of refrigerant and air for each tube. This information facilitates a detailed understanding of the evaporator's performance.

2. DESCRIPTION OF THE EVAPORATOR MODEL

2.1 Modeling Approach

EVAP5 uses a tube-by-tube modeling scheme. That is, the program recognizes each tube as a separate entity for which it calculates heat transfer. These calculations are based on inlet refrigerant and air parameters, properties, and mass flow rates. The simulation begins with the inlet refrigerant tubes and proceeds to successive tubes along the refrigerant path. At the outset of the simulation, the air temperature is only known for the tubes in the first row and has to be estimated for the remaining tubes. A successful run requires several passes (iterations) through the refrigerant circuitry, each time updating inlet air and refrigerant parameters for each tube.

International Congress of Refrigeration, 20th. IIR/IIF. Proceedings.
September 19-24, 1999, Sydney, Australia, 1-7 pp, 1999.

2.2 Heat and Mass Transfer Algorithms

Heat transfer calculations start by calculating the heat-transfer effectiveness, ε, by one of the applicable relations (Kays and London, 1984). With the air temperature changing due to heat transfer, the selection of the appropriate relation for ε depends on whether the refrigerant undergoes a temperature change during heat transfer. Once ε is determined, heat transfer from air to refrigerant is obtained using eq. (1).

$$Q_a = m_a C_{pa}(T_{ai} - T_{ri})\varepsilon \tag{1}$$

The overall heat-transfer coefficient, U, is calculated by eq. (2), which sums up the individual heat-transfer resistances between the refrigerant and the air.

$$U = \left(\frac{A_o}{h_i A_{pi}} + \frac{A_o X_p}{A_{pm} K_p} + \frac{1}{h_l} + \frac{A_o}{A_{po} h_{pf}} + \frac{1}{h_o (1+\alpha)\left(1 - \frac{A_f}{A_o}(1-\phi)\right)} \right)^{-1} \tag{2}$$

The first term of eq. (2) represents the refrigerant-side convective resistance. The second term is the conductive heat-transfer resistance through the tube wall, and the third term accounts for the conduction resistance through the water layer on the fin and tube. The fourth term represents the contact resistance between the outside tube surface and the fin collar. The fifth term is the convective resistance on the air side where the multiplier $(1+\alpha)$ in the denominator accounts for the latent heat transfer on the outside surface. For a dry tube $\alpha = 0.0$ and $1/h_l = 0.0$.

Once the heat transfer rate from the air to the refrigerant is calculated, the tube wall and fin surface temperatures can be calculated directly using heat-transfer resistances. Then, the humidity ratios for the saturated air at the wall and fin temperatures are calculated, and mass transfer from the moist air to the tube and fin surfaces is determined using eq. (3).

$$\Delta\omega = (\omega_{ai} - \omega_w)\left(1 - \exp\left(\frac{-h_o A_{po}}{\mathrm{Le} C_{pa} m_a}\right)\right) + (\omega_{ai} - \omega_{fm})\left(1 - \exp\left(\frac{-h_o A_f}{\mathrm{Le} C_{pa} m_a}\right)\right) \tag{3}$$

The first term in eq. (3) calculates the mass transfer from the air to the tube wall. The second term calculates the mass transfer from the air to the fin surface.

2.3 Refrigerant Distribution

In a heat exchanger with multiple circuits, refrigerant distributes itself in appropriate proportions so that the refrigerant pressure drop from inlet to outlet is the same for all circuits. This observation is the basis of the equation for calculating the fraction of total refrigerant mass flow rate flowing through a particular circuit. This equation, derived from the Pierre pressure drop correlation, has the following form (Domanski, 1991):

$$F_i = \frac{m_i}{m_{tot}} = \frac{1}{\sum_{j=first}^{last} \left(R_i / R_j\right)^{0.571}} \tag{4}$$

where $R_i = \Delta P_i / \Delta G_i^{1.75}$ is the flow resistance for the circuitry branch for which F_i is calculated, and $R_j = \Delta P_j / \Delta G_j^{1.75}$ is the total flow resistance for all circuitry branches originating from a given split point. At the outset of the first iteration loop, the model estimates the i^{th} circuit resistance, R_i, assuming the same flow resistance in each tube regardless of flow quality. Thus, the initial values

of R_i depend on the number of tubes in a given circuit and the circuit's layout (circuit split points and their locations). For subsequent iterations, the values of R_i and F_i are updated using the pressure drops calculated in the previous iteration. Over the course of the simulation, refrigerant distribution is updated and ΔP_i become identical for all branches originating from the same split point.

2.4 Heat Transfer and Pressure Drop Correlations

The model uses the following correlations for calculating heat transfer and pressure drop. Air Side: heat-transfer coefficient for flat fins : Gray and Webb (1986); heat-transfer coefficient for wavy fins: Webb (1990); heat-transfer coefficient for lanced fins: Nakayama and Xu (1983); fin efficiency: Schmidt method (McQuiston and Parker, 1982); heat-transfer coefficient for tube/fin collar junction: Sheffield et al. (1988). Refrigerant Side: single-phase heat-transfer coefficient, smooth tube: McAdams (ASHRAE, 1993); evaporation heat-transfer coefficient up to 80 % quality, smooth tube: Jung and Didion (1989); mist flow, smooth and rifled tubes: linear interpolation between heat-transfer coefficient values for 80 % and 100 % quality; single-phase pressure drop, smooth tube: Petukhov (1970); two-phase pressure drop, smooth tube: Pierre (1964); single-phase pressure drop, return bend, smooth tube: White (Schlichting, 1968); two-phase pressure drop, return bend, smooth tube: Chisholm (Bergles *et al.*, 1981).

The Sheffield correlation for the tube-collar junction heat-transfer coefficient is included in the calculation scheme (eq. (2)) because 10 out of 16 heat exchangers used for the development of the flat fin correlation (Gray and Webb, 1986) were metallurgically bonded, which practically eliminates the fin-to-collar heat-transfer resistance. On the refrigerant side, for a rifled tube, the heat-transfer coefficient and pressure drop are calculated by applying a 1.9 and 1.4 multiplier, respectively, to the values obtained for a smooth tube (Schlager *et al.*, 1989).

2.5 Model Verification

Figure 1 presents a comparison of simulation and test results for an R-22 evaporator at four different inlet air velocity profiles. The tests were performed at 26.6 °C air dry-bulb temperature and 51 % relative humidity. Refrigerant conditions at the evaporator outlet were 7.1 °C saturation temperature and 5.0 °C superheat (Domanski, 1991). The inlet air velocity profile coded as EV90 was the most uniform, and the EV25 velocity profile was the most non-uniform. Figure 1 shows that the model was able to correctly predict the degradation trend in evaporator capacity with increasing maldistribution of the inlet air. These validation results provide confidence in detailed predictions, which are discussed for hypothetical examples in the following section.

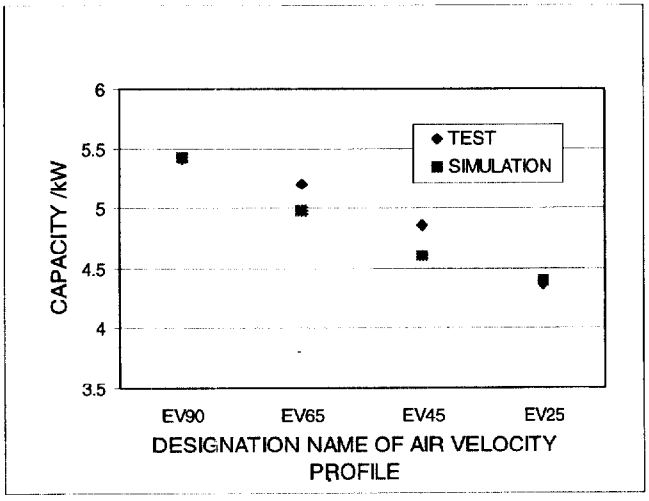

Figure 1: Model validation for different inlet air distributions

3. VISUAL REPRESENTION OF SIMULATION INPUT AND OUTPUT

The visual interface enhances the utility of the model by facilitating preparation of the input data and interpretation of simulation results. Figure 2 shows a side-view schematic of an evaporator indicating the refrigerant path through the heat exchanger and the air velocity profile. Each circle represents a tube in the assembly. The solid lines connecting the tubes denote returning bends located on the near (visible) side, and the dotted lines denote the returning bends on the far side. In this example, the refrigerant enters the evaporator through tube #22. After passing through tube #36, the refrigerant splits into two branches (to tubes #34 and #37), which causes the refrigerant to the exit tubes #1 and #14, respectively. The air flows from the bottom up with the distribution indicated in the figure. The refrigerant circuitry and air distribution were specified using a computer mouse. When a simulation run is completed, detailed refrigerant and air data for each tube can be displayed on a view similar to that in Figure 2. The parameters include inlet and outlet air and refrigerant temperatures, refrigerant quality, enthalpy, entropy, pressure drop, and refrigerant mass flow rate fraction flowing through each tube.

Figure 3 presents selected simulation results for the heat exchanger shown in Figure 2. The simulation was performed for 5 °C refrigerant saturation temperature at the evaporator exit manifold and 7 °C refrigerant superheat. Inspection of the detailed results indicates that the refrigerant branch ending with tube #1 is flooded, and the branch ending with tube #14 has a superheated vapor in the last nine tubes. This can be confirmed by observing refrigerant temperature at the outlet of each tube. The bottom side-view schematic in Figure 3 provides the complementary information on the air temperature past each tube. Since the refrigerant temperatures in the tubes with superheated refrigerant (tubes #12, #26, #40, #41, #42, #28, #27, #13, and #14) approach the air inlet temperature, minimal heat transfer takes place in the right-side section, which produces outlet air temperatures above 20 °C. This result is due to the fact the velocity profile imposed in Figure 2 provides approximately two-thirds of the air flow to the right-side section of the evaporator.

Figure 4 presents simulation results for the evaporator with a modified refrigerant circuit design to accommodate the maldistributed inlet air. Specifically, an additional refrigerant split was introduced after tube #25. This modification allowed 64.5 % of the total refrigerant mass flow to flow to the right side of the evaporator (compared to 41 % in the original circuitry design shown in Figure 3). This resulted in a balanced refrigerant circuitry and a 26 % improvement in evaporator capacity.

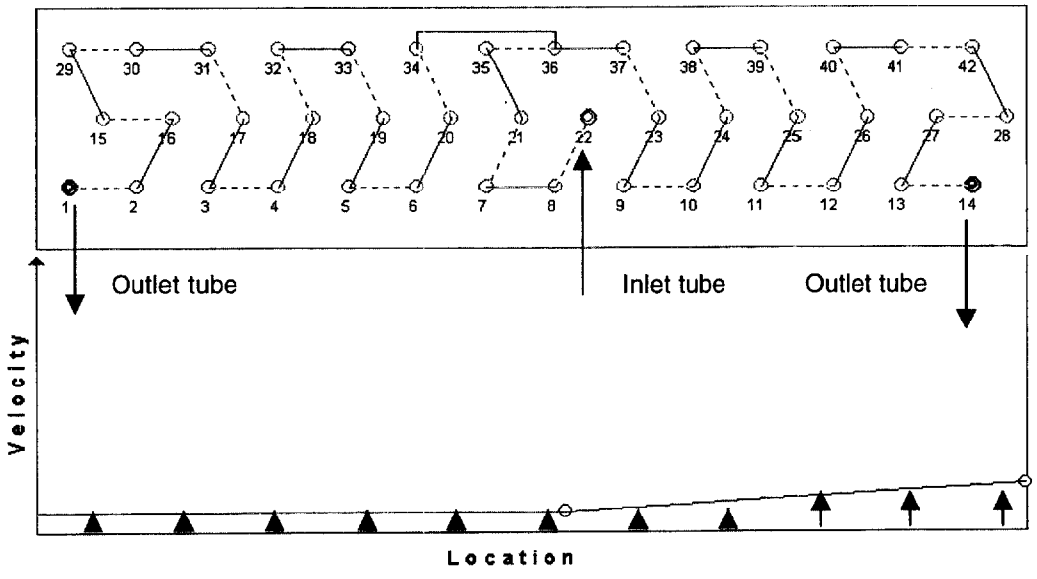

Figure 2: Side view of evaporator with circuitry specification and air velocity profile

Air		Refrigerant		Results	
Inlet temperature (C)	25.0	Outlet sat. temp. C	5.0	Total capacity (kW)	3.00
Inlet pressure (kPa)	101.325	Superheat C	7.00	Sensible capacity (kW)	1.88
Inlet relative humidity (fraction)	0.5	Mass flow rate (kg/h)	64.700	Latent capacity (kW)	1.12
Vol. flow rate (m^3/min)	10.00				

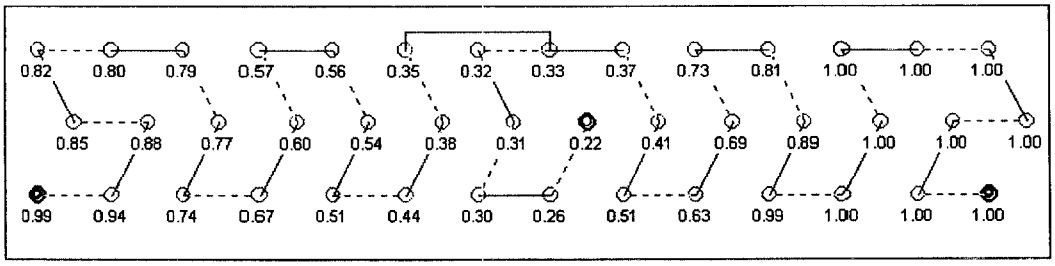

Refrigerant outlet quality (%)

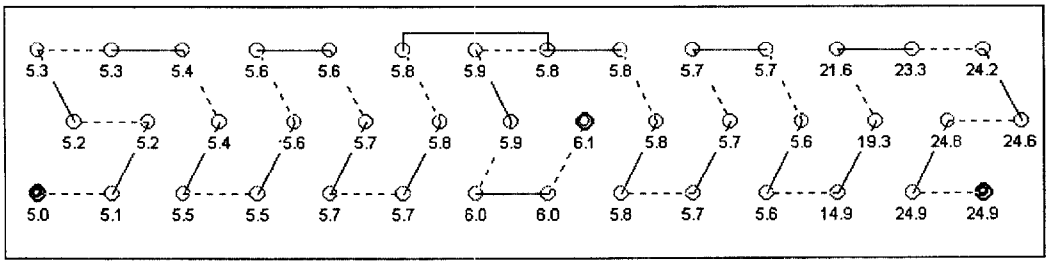

Refrigerant outlet temperature (°C)

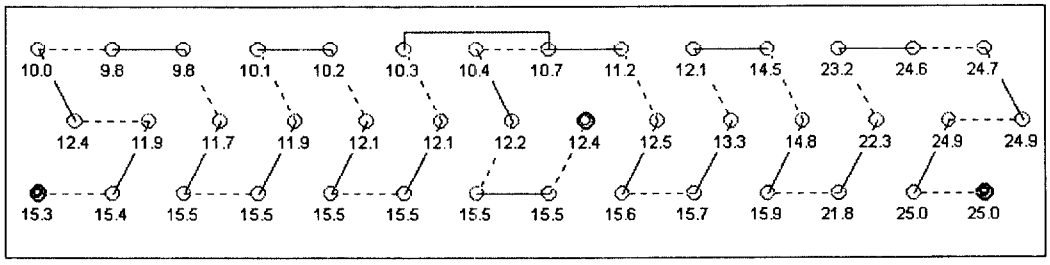

Air outlet temperature (°C)

Figure 3: Global and detailed simulation results

Figure 5 shows outlet tube refrigerant temperatures for R-407C (zeotropic mixture) in an evaporator with the circuitry of Figure 2 and a uniform velocity profile. Figure 5 shows a temperature glide throughout the circuitry. This display of refrigerant temperatures can be particularly helpful when attempting to optimize the circuitry design for zeotropic mixtures.

4. FUTURE WORK

Several upgrades will improve the model; some of them are currently being implemented and others are envisioned for the future. The model is in the process of being updated with the latest heat transfer and pressure drop correlations. Although the EVAP5 model increases a designer's ability to optimize refrigerant circuitry for a non-uniform air distribution, the task remains a challenging one. To ease this design problem, work is underway to develop a genetic algorithm and symbolic learning module capable of producing optimized refrigerant circuit architectures. When simulating evaporator performance with zeotropic mixtures, the need to address heat transfer via fins between neighboring tubes having different temperature becomes very important. Splitting individual tubes into smaller segments for heat transfer calculations would also improve the model.

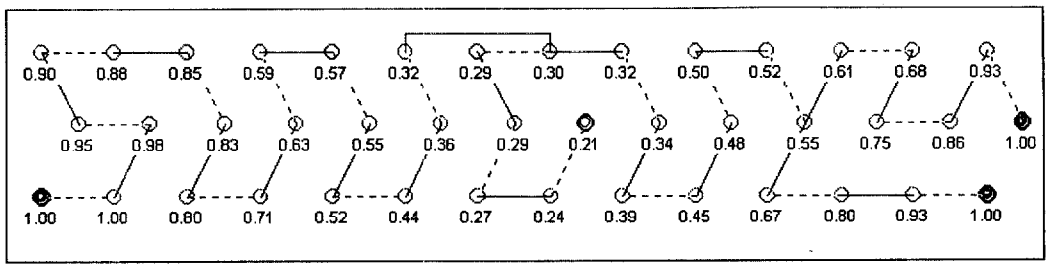

Refrigerant outlet quality (%)

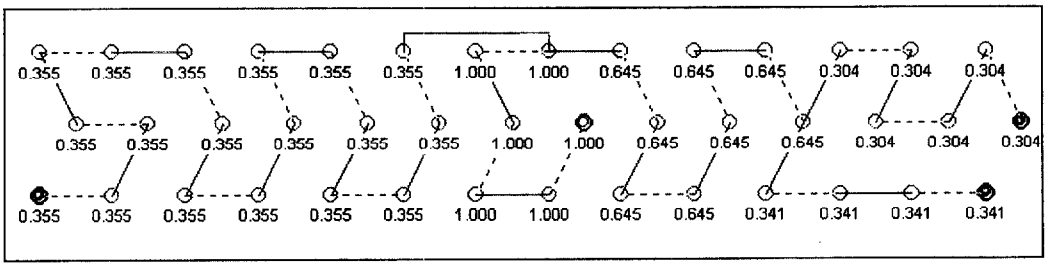

Refrigerant distribution (fraction)

Figure 4: Detailed simulation results for a modified circuitry

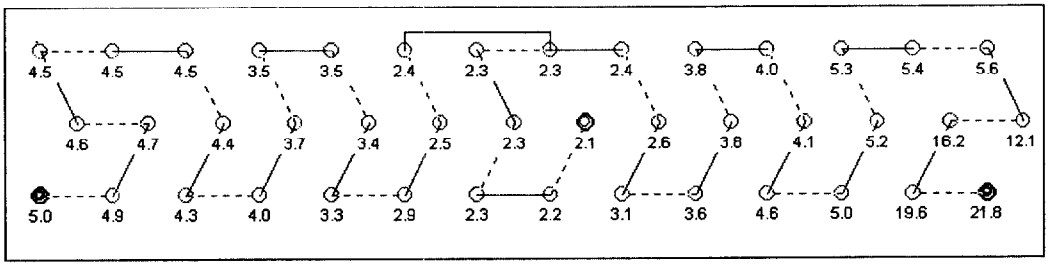

Refrigerant outlet temperature (°C)

Figure 5: Refrigerant outlet temperatures for simulations with R-407C zeotropic mixture

5. NOMENCLATURE

A = surface area (m^2)
C_{pa} = specific heat at const. pressure for air (kJ/(kg °C))
F_i = m_i/m_{total}, fraction of total refrigerant mass flow rate flowing through i^{th} circuit (-)
G_i = refrigerant mass flux for i^{th} circuitry branch ($kg/(m^2 s)$)
h_D = air-side mass transfer coeff. ($kg/(m^2 s)$)
h = heat-transfer coefficient ($kW/(m^2 °C)$)
i_{fgw} = latent heat of water (kJ/kg)
K = thermal conductivity (kW/(m °C))
Le = $h_o/(h_D \cdot C_{pa})$, Lewis number (-)

m = mass flow rate (kg/s)
P = pressure (kPa)
Q_a = heat-transfer rate for a given tube calculated on the air side (kW)
R_i, R_j = flow resistance offered by a given branch leaving a split (it accounts for the effects of tube geometry, fluid density and viscosity) ($kN\ m^{2.5}/(kg/s)^{1.75}$)
T = temperature (°C)
U = overall heat-transfer coeff. ($kJ/(m^2 °C)$)
X_p = thickness of tube wall (m)

α = $i_{fgw}(\omega_a - \omega_w)/(C_{pa}(T_a - T_w))$ (-)
ε = heat-transfer effectiveness (-)

ϕ = fin efficiency (-)
ω = humidity ratio ($kg_w/kg_{a,dry}$)

ω_{fm} = humidity ratio of saturated air at mean temp. of condensate wetting the fin ($kg_w/kg_{a,dry}$)
ω_w = humidity ratio of saturated air at temp. of condensate wetting the tube ($kg_w/kg_{a,dry}$)

Subscripts:

a = air	l = latent, condensate, or frost	p = tube
f = fin	m = mean	r = refrigerant
i = inlet, inside tube, or i^{th}	o = outlet or outside (air-side)	w = water or tube wall

6. REFERENCES

1. ASHRAE, 1993, *ASHRAE Handbook*, Fundamentals Volume, p. 3.14, American Society of Heating, Refrigerating and Air Conditioning Engineers, Inc., Atlanta, GA.
2. Bergles, A.E., Collier, J.G., Delhaye, J.M., Hewitt, G.F., and Mayinger, F., 1981, *Two-Phase Flow and Heat Transfer in the Power and Process Industries*, p. 146-147, Hemisphere Publishing Corp., New York, NY.
3. Chi, J., 1979, *A Computer Model HTPUMP for Simulation of Heat Pump Steady-State Performance*, National Bureau of Standards, Internal Report, Washington, D.C.
4. Domanski, P.A., Didion, D.A., 1983, Computer Modeling of the Vapor Compression Cycle with Constant Flow Area Expansion Device, *Building Science Series 155*, National Bureau of Standards, Gaithersburg, MD.
5. Domanski, P.A., 1991, Simulation of an Evaporator with Nonuniform One Dimensional Air Distribution, *ASHRAE Transactions*, Paper No. NY-91-13-1, Vol. 97, Part 1.
6. Gallagher, J., McLinden, M.O., Morrison, G., Huber, M., 1996, *NIST Standard Reference Database 23*, Version 5.0 (REFPROP), National Institute of Standards and Technology, Gaithersburg, MD.
7. Gray, D.L., Webb, R.L., 1986, Heat Transfer and Friction Correlations for Plate Finned-Tube Heat Exchangers Having Plain Fins, *Proc. of Eighth Int. Heat Transfer Conference*, San Francisco.
8. Jung, D.S., Didion, D.A., 1989, *Horizontal Flow Boiling Heat Transfer using Refrigerant Mixtures*, ER-6364, EPRI Project 8006-2.
9. Kays, W.M., London, A.L., 1984, *Compact Heat Exchangers*, McGraw-Hill.
10. Lee, J., Domanski, P. A., 1997, *Impact of Air and Refrigerant Maldistributions on the Performance of Finned-Tube Evaporators with R-22 and R-407C*, Report DOE/CE/23810-81 for ARI, National Institute of Standards and Technology, Gaithersburg, MD.
11. Nakayama, W., and Xu, L.P., 1983, Enhanced Fins for Air-Cooled Heat Exchangers Heat Transfer and Friction Factor Correlations, *Proc. of ASME-JSME Thermal Engineering Joint Conference*, p. 495, ASME, New York.
12. McQuiston, F.C., and Parker, J.D, 1982, *Heating, Ventilating, and Air Conditioning*, J.Wiley & Sons.
13. Petukhov, B.S., 1970, Heat transfer and friction in turbulent pipe flow with variable physical properties, *Advances in Heat Transfer*, Vol. 6., p. 503-564, Academic Press, New York.
14. Pierre, B., 1964, Flow Resistance with Boiling Refrigerants, *ASHRAE Journal*, September issue.
15. Schlichting, H., 1968, *Boundary-Layer Theory*, Sixth Edition, p. 590, McGraw-Hill, Inc.
16. Schlager, L.M., Pate, M.B., Bergles, A.E., 1989, Heat Transfer and Pressure Drop during Evaporation and Condensation of R-22 in Horizontal Micro-fin Tubes, *Int. J. Refrig.*, Vol. 12, No. 1.
17. Sheffield, J.W., Wood, R.A., Sauer, H.J., 1988, Experimental Investigation of Thermal Conductance of Finned Tube Contacts, *Experimental Thermal and Fluid Science*, Elsevier Science Publishing Co., Inc., New York, NY.
18. Webb, R.L., 1990, Air-Side Heat Transfer Correlation for Flat and Wavy Plate Fin-and-Tube Geometries, *ASHRAE Transactions*, Paper No. SL-90-1-2, Vol. 96, Part 2.

7. ACKNOWLEDGEMENTS

The author wishes to acknowledge J.H. Lee (L.G. Electronics) who introduced several modifications to the EVAP5 during his tenure as a guest researcher at NIST in 1997. The visual interface was developed by J. Wnek (independent consultant, Germantown, MD) and J. Michalski (G. Mason University). J. Gebbie (NIST), V. Payne (NIST), and S. Palmer (U.S. Naval Academy) provided comments on the original manuscript. Partial funding for recent EVAP5 upgrades was provided by ARTI under ARTI MCLR Project No. 665-54500 managed by G. Hourahan.

MODEL EVAPORATEUR AVEC UNE INTERFACE VISUEL

RESUME: Ce papier présente un model d'évaporateur et son utilité lorsqu'il est équipe d'une interface visuel. Le shéma de ce model est un "tube par tube" et accepte une distribution de réfrigirant entre différent circuits et adaptable pour une difusion d'air non uniforme. L'interface facilite la spécification complexe des circuits réfrigirants et la présentation de resultats détailles de simulations pour chaque tube tel que la température , l'enthalpie , l'entropie , la préssion et le pourcentage de flux du réfrigirant.